Available online at www.sciencedirect.com
SCIENCE DIRECT®
PERGAMON
Polyhedron 22 (2003) 1989–1994
POLYHEDRON
www.elsevier.com/locate/poly

Spin density distributions of *p*-*N*-alkylpyridinium nitronyl nitroxides studied by solid-state high-resolution NMR

Goro Maruta [a,*], Sadamu Takeda [a], Akira Yamaguchi [b], Tsunehisa Okuno [b], Kunio Awaga [c]

[a] *Division of Chemistry, Graduate School of Science, Hokkaido University, Sapporo 060-0810, Japan*
[b] *Department of Basic Science, Graduate School of Arts and Sciences, The University of Tokyo, Tokyo 153-8902, Japan*
[c] *Division of Chemistry, Graduate School of Science, Nagoya University, Nagoya 464-8602, Japan*

Received 6 October 2002; accepted 3 January 2003

Abstract

The electron spin density distributions of *p*-*N*-alkylpyridinium α-nitronyl nitroxides with alkyl = methyl (*p*-MPYNN) and *n*-butyl (*p*-BPYNN) were determined in their iodide salts from the temperature dependence of the solid-state high-resolution ^{1}H MAS NMR spectra. The results were compared with that of *p*-pyridyl α-nitronyl nitroxide (*p*-PYNN) to see how positive charge on the aromatic ring affects the spin density distribution. This effect was not significant contrary to the effect of incorporation of a nitrogen atom into the aromatic group. The change in the magnitude of the spin density can be ascribed to the dihedral angle between nitroxide and aromatic moieties. Relatively large hyperfine coupling constant of *N*-methyl proton, which is almost half as large as those of β-methyl proton, implies the utility of the *N*-methyl group as an intermolecular magnetic coupler.

Keywords: Organic magnetism; Nitronyl nitroxide radical; ^{1}H MAS NMR; Fermi contact shift; Electron spin density distribution; DFT calculation

1. Introduction

Since the discovery of the first organic ferromagnet *p*-NPNN (2-(4′-nitrophenyl)-4,4,5,5-tetramethyl-4,5-dihydro-1*H*-imidazol-1-oxyl-3-oxide) [1], the magnetism of aryl nitronyl nitroxide crystals has attracted much interest [2]. Spin density distribution of the aromatic moiety of aryl nitronyl nitroxide is important from the viewpoint of intermolecular magnetic interaction in the crystalline phase, since the π-conjugated aromatic ring of the stable radical is considered as a magnetic coupler between adjacent radical molecules [3,4]. It is desired to clarify the effect of the chemical modification on rearrangement of the electron spin density distribution for designing aryl nitronyl nitroxide to produce novel organic magnetic materials.

In this paper, we report the hyperfine coupling constants (hfcc) of the protons of *p*-*N*-alkylpyridinium α-nitronyl nitroxides with alkyl = methyl (*p*-MPYNN) and *n*-butyl (*p*-BPYNN) (see Scheme 1) in their iodide salts determined from the temperature dependence of the Fermi contact shifts of protons measured by high speed (~ 15 kHz) magic angle spinning (MAS) NMR. We also performed theoretical calculations of the hfcc of these compounds at UBLYP/EPR-II level [5–7] and discuss the spin polarization mechanism of the heterocyclic μ-conjugated systems on the basis of spin density distribution. NMR and DFT results were compared with those of *p*-pyridyl nitronyl nitroxide (*p*-PYNN) [8,9].

2. Method

Static proton NMR spectrum of paramagnetic polycrystalline specimen exhibits broad width due to the dipole interaction between the nuclear spin and electron spins [10]. MAS technique averages the interaction in

* Corresponding author. Tel.: +81-11-706-3505; fax: +81-11-706-4841.
E-mail address: maruta@sci.hokudai.ac.jp (G. Maruta).

0277-5387/03/$ - see front matter © 2003 Published by Elsevier Science Ltd.
doi:10.1016/S0277-5387(03)00292-4

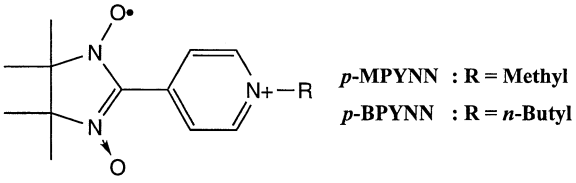

Scheme 1.

principle and provides the isotropic shift of the NMR absorption line. The observed isotropic shift δ_{iso} on a ppm scale consists of the paramagnetic contact term and the temperature independent diamagnetic term δ_{dia}. The anisotropy of the g-value as well as the Fermi contact interaction contributes to the paramagnetic term.

$$\delta_{iso} = \frac{A_H}{\gamma_H/2\pi}\frac{\chi_M}{N_A g \mu_B} + \delta_{dia} \quad (1)$$

$$A_H = A_{Fermi} + A_{pseudo} \quad (2)$$

where A_{Fermi} and A_{pseudo} are respectively the Fermi and the pseudo contact coupling constant of the proton in Hz, T is the absolute temperature, χ_M is the molar susceptibility of the radical, N_A is the Avogadro constant, and the other terms have their usual meanings [11,12]. In Eq. (1), g represents averaged g-value, $(g_{xx} + g_{yy} + g_{zz})/3$. The anisotropy of g-value is very small for typical organic radical crystals, e.g. the principal values of the g-tensor of phenyl nitronyl nitroxide radical fall in the range 2.00620 ± 0.0040 [13]. Thus in our case, A_{pseudo} is estimated to be less than 0.01 MHz and can be neglected relative to A_{Fermi}. The plot of observed isotropic shift against inverse temperature gives the hfcc A_H which is proportional to the electron spin density $\rho(R_H)$ at the proton position R_H as follows [11]:

$$A_H \cong A_{Fermi} = \frac{8\pi}{3} g \mu_B \frac{\gamma_H}{2\pi} \rho(R_H) \quad (3)$$

3. Experimental

Preparation of p-RPYNN$^{\bullet}$I has been previously reported [14]. Proton high speed MAS NMR spectra were measured by a single pulse method for polycrystalline samples between 180 and 300 K at the resonance frequency of 300.13 MHz with Bruker DSX300 spectrometer and 4 mm CP/MAS probe. $\pi/2$ Pulse length was 1.2 μs. A conventional zirconia rotor with boron nitride cap was used. The specimen ($\approx$ 35–40 mg) was carefully packed at the center of the rotor (4–5 mm long) to achieve homogeneous temperature over the sample and Teflon powder was used as spacer. Dry N_2 gas evaporated from the liquid N_2 container was utilized for the high speed MAS (9–15 kHz).

The thermometer of the MAS probe was calibrated against the isotropic chemical shift of ^{207}Pb MAS NMR spectrum of $Pb(NO_3)_2$ [15]. The obtained temperature coefficient of the isotropic chemical shift of ^{207}Pb 0.784 ppm K^{-1} was almost the same as that reported in Ref. 15 (0.753 ppm K^{-1}). Temperature raise of the specimen as the increase of the spinning rate was also examined and calibrated. Uncertainty of the temperature measurement after the calibration was 4 K and temperature fluctuation during accumulation was within 1 K. All proton NMR shifts were measured from the tetramethylsilane dissolved in CCl_4.

4. Theoretical computation

Electron spin density at position R can be computed as the difference between electron density of α spin and that of β spin [11],

$$\rho(R) = \sum_i^{occ} |\psi_i^{\alpha}(R)|^2 - \sum_i^{occ} |\psi_i^{\beta}(R)|^2 \quad (4)$$

where ψ_i^{α} is an unrestricted molecular orbital for α spin electron and each summation runs over occupied orbitals.

Using GAUSSIAN 98 program package [16], we performed UBLYP/EPR-II calculation on p-MPYNN, p-BPYNN cation and neutral aryl nitronyl nitroxides (aryl = phenyl, pyridyl, and p-n-butylphenyl). All calculation were done for isolated single molecule model. The atomic coordinates were based on crystal structure of p-BPYNN$^{\bullet}$I [14]. Butyl group and pyridyl nitrogen atom of p-BPYNN were changed appropriately to generate the atomic coordinates of the other radicals. The other part of molecular geometry were in common among the five radicals for the purpose of comparing substituent effect on hfcc without modifying geometric parameters such as torsion angle between aromatic ring and nitroxide moiety. The nuclear spin electron spin coupling constants A_{Fermi} were obtained by using Eqs. (3) and (4).

5. Result and discussion

5.1. Assignment of NMR signals

Fig. 1(a) shows proton MAS NMR spectrum of p-MPYNN$^{\bullet}$I at 294 K, in which six isotropic signals were distinguished from the spinning sidebands (SSB). The signals were grouped into two sets, one shifts to higher frequency with decreasing temperature and the other shifts to lower frequency as shown in Fig. 3(a). The temperature dependence of the signals were well interpreted in terms of the signet–triplet model,

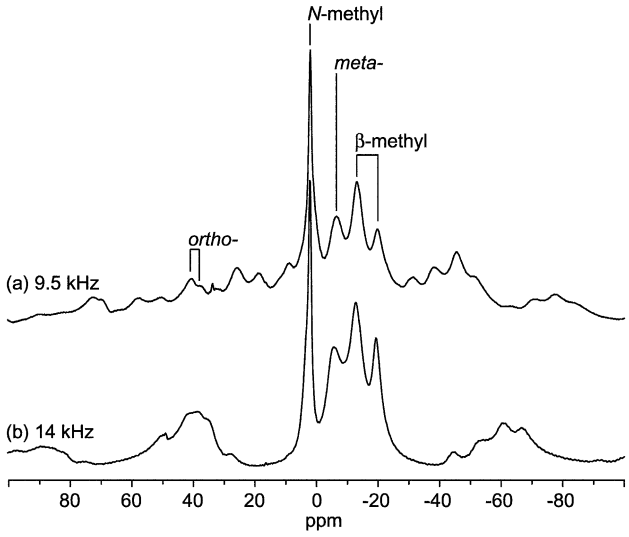

Fig. 1. Proton MAS NMR spectra of polycrystalline *p*-MPYNN•I measured at 294 K and at (a) 9.5 kHz, (b) 14 kHz of the spinning speeds. Peaks without assignment are SSB. Signals of *ortho*-protons overlap SSB of β-methyl groups at 14 kHz of the spinning speed, and vice versa.

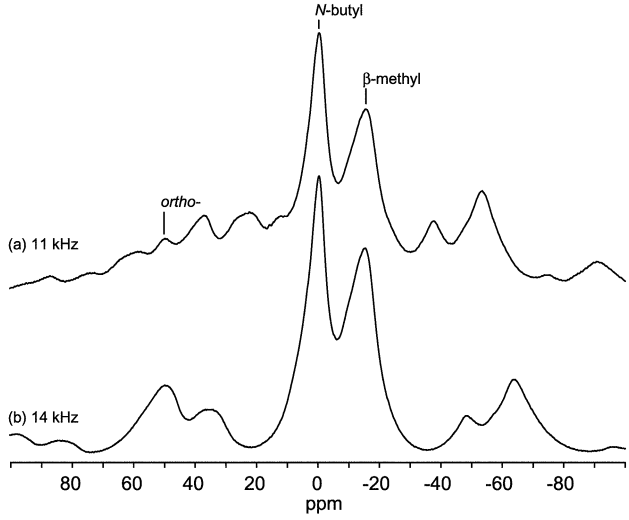

Fig. 2. Proton MAS NMR spectra of polycrystalline *p*-BPYNN•I measured at 294 K and at (a) 11 kHz, (b) 14 kHz of the spinning speeds. Peaks without assignment are SSB. Signals of *ortho*-protons overlap SSB of *N*-butyl groups at 14 kHz of the spinning speed, and vice versa.

$$\chi_M = \frac{C}{T}\frac{4}{3 + \exp(-2J/k_B T)} \quad (5)$$

where $J/k_B = -74$ K and $C = 0.375$ emu K mol^{-1} are the intradimer coupling constant and the Curie constant, respectively, which are determined from susceptibility measurement, and k_B is the Boltzmann constant [14]. The solid curves in Fig. 3(a) were best fit of Eq. (1) with the parameters A_H and δ_{dia} listed in Table 1.

The two signals at higher frequencies (39 and 36 ppm) in Fig. 1(a) were assigned to *ortho*-protons because the

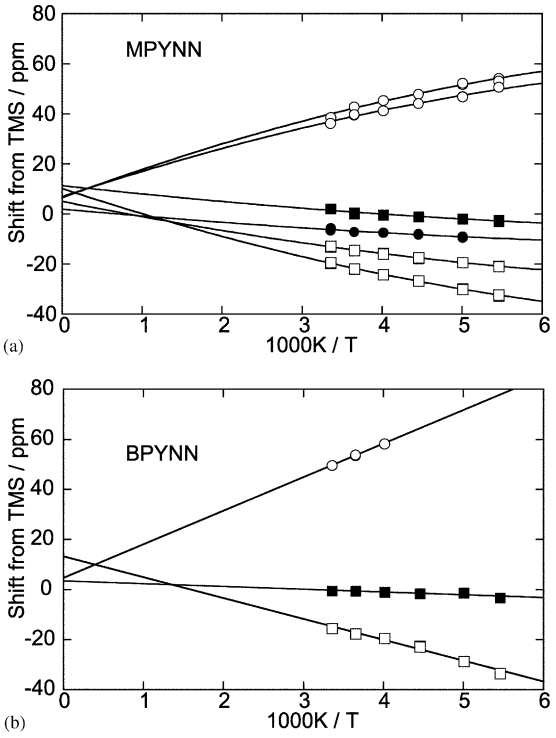

Fig. 3. Temperature dependence of the isotropic ^{1}H NMR shifts in the salts of (a) *p*-MPYNN•I and (b) *p*-BPYNN•I. open circle: *ortho*-, filled circle: *meta*-, open square: β-methyl, filled square: (a) *N*-methyl and (b) *N*-butyl. Solid curves are the results of least-squares fitting (see text).

corresponding signals of *para*- and *ortho*-protons are observed in this spectral region for analogues [9,17]. The two *ortho*-protons in MPYNN•I salt are crystallographically inequivalent [14] so that their hfcc can be different though one-to-one assignment is difficult.

The lower frequency set consists of signals from *meta*-protons, 4,4,5,5-methyl (β-methyl) groups, and *N*-methyl group. The β-methyl groups are divided into equatorial and axial methyl groups. We assumed that the three protons of each methyl group give an averaged signal because of the rapid rotation of the methyl group around its own C_3 axis above 180 K. The signal at 2 ppm in Fig. 1(a) was assigned to *N*-methyl group from its weak SSB which represent small anisotropy. A spectrum measured at higher MAS speed (Fig. 1(b)) also shows that intensity ratio of SSB to isotropic signal at 2 ppm is much smaller than those of other signals. In MPYNN•I salt, *N*-methyl protons have the smallest anisotropy due to electron-proton dipolar interaction, which is in inverse proportion to the cube of the distance between the proton and the unpaired electron, because they are most distant from the radical site. Then, the signal at −6 ppm in Fig. 1(a) were assigned to *meta*-protons and the remaining two signals (−13 and −20 ppm) were assigned to β-methyl groups. This assignment is based on the fact that the signal at −6 ppm broadens out to be buried in the other signals with decreasing

Table 1
Hfcc (A_H/MHz) and diamagnetic shifts (δ_{dia} (ppm)) of protons in nitronyl nitroxides determined from high-resolution solid-state NMR

	p-PYNN [a]		*p*-MPYNN•I		*p*-BPYNN•I	
Proton site	A_H (MHz)	δ_{dia} (ppm)	A_H (MHz)	δ_{dia} (ppm)	A_H (MHz)	δ_{dia} (ppm)
ortho-H	1.59	3.8	1.49	6.5	1.70	4.6
			1.34	5.9		
meta-H	−0.56	13.4	−0.34	1.9	not observed	
N-Alkyl-H			−0.44	11.3	ca. −0.14	3.5
β-Methyl-H	−0.96	7.5	−0.81	5.0	−1.06	13.2
			−1.33	10.1		
Torsion angle [b]	23°		28°		6°	

[a] Ref. [9].
[b] Torsion angle between aryl group and nitroxide moiety.

temperature as shown in Fig. 4. This behavior suggests that this signal consists of unresolved two (or more) signals and the signal is much weaker than the remaining two signals in intensity, and can be interpreted with the above assignment: the signals from inequivalent *meta*-protons can be distinct as well as those of *ortho*-protons and the ratio of the number of protons is *meta*:equatorial methyl:axial methyl = 2:6:6. There is, however, another interoperation that the last three signals all came from methyl groups and the signals of *meta*-protons are lost in those of twelve methyl protons though in this assignment it is unclear why the signal at −6 ppm disappears at low temperature. Another experiment such as deuterium NMR of selectively deuterated sample [18] is needed to rule out the alternative assignment.

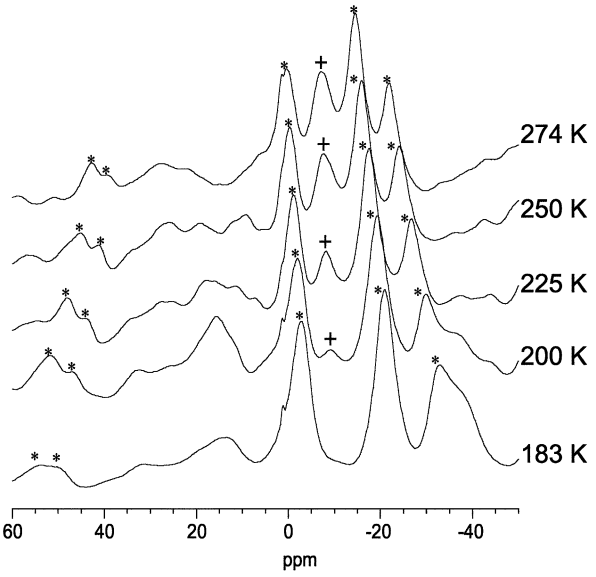

Fig. 4. Temperature dependence of the proton MAS NMR spectrum of *p*-MPYNN•I. The signal of *meta*-proton, indicated by plus sign, disappears below 200 K. Asterisks indicate the signals of the other proton. Peaks with no mark are SSB. Each spectrum was obtained as follows: two or three spectra were taken at different spinning speeds (9–11 kHz) at each temperature, then these spectra were arithmetically multiplied to increase the ratio of signal to SSB.

Fig. 2 shows proton MAS NMR spectra of *p*-BPYNN•I at 294 K. Three isotropic signals were distinguished from the SSB and assigned to *ortho*-protons, *N*-butyl group, and β-methyl groups as shown in Fig. 2. The assignments for *ortho*-protons, *N*-butyl group are based on the same hypothesis as those of *p*-MPYNN•I, while the signals of *meta*-protons are missing in large signals from *N*-butyl group and β-methyl groups in the spectra of *p*-BPYNN•I. Fig. 3(b) shows the isotropic NMR shifts proportional to reciprocal temperature and best fit of Eq. (1) with the parameters A_H and δ_{dia} listed in Table 1, using

$$\chi_M = \frac{0.375\ \text{emu K mol}^{-1}}{T} \tag{6}$$

where we neglected the small intermolecular magnetic interaction ($J/k_B < 1$ K) in *p*-BPYNN•I salt [14].

5.2. DFT calculation of the radicals

Hfcc of aryl protons in the nitronyl nitroxides are calculated at the level of UBLYP/EPR-II (Table 2). The atomic coordinates used in the calculation are all based on *p*-BPYNN molecule in *p*-BPYNN•I salt determined by X-ray diffraction [14]. Hence, the change of the hfcc

Table 2
Hfcc (A_H (MHz)) of aryl protons in nitronyl nitroxides by DFT calculation[a]

Aryl group	*ortho*-H	*meta*-H
Phenyl	1.02	−0.32
p-Pyridyl	1.06	−0.25
p-n-Butyl-phenyl	1.00	−0.30
p-Methyl-pyridinium	1.00	0.04
p-n-Butyl-pyridinium	1.00	−0.01

[a] At the level of UBLYP/EPR-II for isolated single molecule of which atomic coordinate is based on *p*-BPYNN radical in *p*-BPYNN•I [14].

with the aryl group is caused by the substitution. The incorporation of a nitrogen atom at *para*-position increases the hfcc of *ortho*-proton and decreases that of *meta*-proton in magnitude. This result is the same as that obtained in the previous study [9]. DFT and NMR results are in good agreement for *p*-PYNN. The theoretical values of hfcc of *meta*-protons of the two radical cations are very different from those of the neutral radicals. For *p*-MPYNN, the calculated value is positive and in disagreement with the present NMR result. We also calculated hfcc using the atomic coordinate based on the crystal structure of *p*-MPYNN$^{\bullet}$I that is used for the NMR measurement, nevertheless the same theoretical result was obtained. For *p*-BPYNN, the calculated hfcc of *meta*-proton was negative but very small compared with those of *p*-PYNN and phenyl nitronyl nitroxide. For *p*-*n*-butyl-phenyl nitronyl nitroxide that is a neutral analogue of *p*-BPYNN cation radical, the change of hfcc from phenyl nitronyl nitroxide was small at the same level of calculation. The present DFT calculation suggests that the hfcc of *meta*-proton changes drastically by substitution of the phenyl group for *p*-alkylpyridinium. This is noteworthy because if the nitrogen atom of the pyridinium ring is at *meta*-position referred to nitronyl nitroxide group, the spin density distribution calculated by DFT method is essentially the same as that of *meta*-alkylphenyl group [19]. The present NMR experiment on *p*-MPYNN$^{\bullet}$I contradicts the theoretical calculation as mentioned above. However, NMR signal of *meta*-proton was not observed for *p*-BPYNN$^{\bullet}$I and there is still room for another interpretation of the spectrum of *p*-MPYNN$^{\bullet}$I. We are planning deuterium NMR measurement of selectively deuterated sample to find whether the spin density distribution of *p*-MPYNN radical cation is unusual.

5.3. Spin density distribution of the radicals

There is no experimental evidence for the peculiar spin density distribution predicted by the theoretical calculation. In this section, we discuss the spin density distribution of *p*-alkyl-PYNN radical cation on the basis of NMR result.

We observed two NMR signals of β-methyl groups of *p*-MPYNN. The five-membered ring of the nitronyl nitroxide moiety in the cation exhibits half-chair conformation where four methyl groups are divided into axial and equatorial groups [14]. It is well known that spin density of the axial methyl carbon is larger than that of the equatorial methyl carbon [20]. This is not true for the methyl protons because one of the three protons of the axial methyl group bears positive spin density [18]. The hfcc averaged over the three protons, thus, may be positive or negative and can be a smaller negative value than those of equatorial methyl groups. The averaged hfcc of β-methyl proton is not in proportional to the spin density of the methyl carbon atom.

The hfcc of *N*-methyl group of *p*-MPNN is −0.44 MHz and its absolute value is smaller than those of β-methyl groups and *ortho*-proton. From the viewpoint of intermolecular magnetic interaction through hydrogen atom, it is noteworthy that the mechanism of the hyperfine coupling between unpaired electron and *N*-methyl protons differs from the couplings between the electron and the other protons [21]. On the one hand, β-methyl protons, except for the proton bearing positive hfcc, and *ortho*-proton couple to the unpaired electron indirectly through spin polarized C–H bond formed with their adjacent carbon atoms. On the other hand, negative spin density of *N*-methyl group results from hyperconjugation with aromatic carbon atoms including α-carbon atom that lies between nitroxide nitrogen atoms. Experimentally observed negative hfcc of *N*-methyl group is evidence that the hyperconjugation expands the frontier orbital polarizing π electrons of α- and *ortho*-carbon atoms and *para*-pyridinium nitrogen atom toward *N*-methyl hydrogen atoms. Consequently, the intermolecular magnetic interaction through this *N*-methyl hydrogen atoms can be more effective than that through another hydrogen atom on which s-electron is polarized by the neighboring carbon atom via local exchange interaction. For this reason, *N*-methyl group is expected to be a good magnetic coupler though its hfcc is not particularly large.

Finally, we discuss the amplitude change of *ortho*-proton among *p*-PYNN, *p*-MPYNN, and *p*-BPYNN. The change is attributable to the torsion angle φ (listed in last row of Table 1) between aryl group and nitronyl nitroxide moiety. The hfcc of ring protons is expected to be in proportional to $\cos^2\varphi$ Table 1 shows that the hfcc of *ortho*-proton decreases monotonously with torsion angle φ. Substituent effect caused by attachment of alkyl group to pyridyl nitrogen atom is not significant among these three radicals.

Acknowledgements

This research was supported by The Mitsubishi Foundation and by grant-in-aid for Scientific Research on Priority Areas (A) from the Ministry of Education, Culture, Sports, Science and Technology of Japan.

References

[1] M. Kinoshita, P. Turek, M. Tamura, Y. Nozawa, D. Shiomi, Y. Nakazawa, M. Ishikawa, M. Takahashi, K. Awaga, T. Inabe, Y. Maruyama, Chem. Lett. (1991) 1225.
[2] T. Sugawara, A. Izuoka, Mol. Cryst. Liq. Cryst. 305 (1997) 41.
[3] H.M. McConnell, J. Chem. Phys. 39 (1963) 1910.

[4] A. Oda, T. Kawakami, S. Takeda, W. Mori, Y. Hosokosi, M. Tamura, M. Kinoshita, K. Yamaguchi, Mol. Cryst. Liq. Cryst. 306 (1997) 331.
[5] A.D. Becke, Phys. Rev. A 38 (1988) 3098.
[6] C. Lee, W. Yang, R.G. Parr, Phys. Rev. B 37 (1988) 785.
[7] V. Barone, in: D.P. Chong (Ed.), Recent Advances in Density Functional Methods Part I, World Scientific, Singapore, 1995, p. 287.
[8] K. Awaga, T. Inabe, Y. Maruyama, Chem. Phys. Lett. 190 (1993) 349.
[9] G. Maruta, S. Takeda, A. Yamaguchi, T. Okuno, K. Awaga, K. Yamaguchi, Mol. Cryst. Liq. Cryst. 334 (1999) 295.
[10] D. Ondercin, T. Sandreczki, R.W. Kreilick, J. Magn. Reson. 34 (1979) 151.
[11] H.M. McConnell, D.B. Chesnut, J. Chem. Phys. 28 (1958) 107.
[12] R.J. Kurland, B.R. McGarvey, J. Magn. Reson. 2 (1970) 286.
[13] J.A. D'Anna, J.H. Wharton, J. Chem. Phys. 53 (1970) 4047.
[14] K. Awaga, A. Yamaguchi, T. Okuno, T. Inabe, T. Nakamura, M. Matsumono, Y. Maruyama, J. Mater. Chem. 4 (1994) 1377.
[15] A. Bielecki, D.P. Burum, J. Magn. Reson. Ser. A 116 (1995) 215.
[16] M.J. Frisch, G.W. Trucks, H.B. Schlegel, G.E. Scuseria, M.A. Robb, J.R. Cheeseman, V.G. Zakrzewski, J.A. Montgomery, Jr., R.E. Stratmann, J.C. Burant, S. Dapprich, J.M. Millam, A.D. Daniels, K.N. Kudin, M.C. Strain, O. Farkas, J. Tomasi, V. Barone, M. Cossi, R. Cammi, B. Mennucci, C. Pomelli, C. Adamo, S. Clifford, J. Ochterski, G.A. Petersson, P.Y. Ayala, Q. Cui, K. Morokuma, P. Salvador, J.J. Dannenberg, D.K. Malick, A.D. Rabuck, K. Raghavachari, J.B. Foresman, J. Cioslowski, J.V. Ortiz, A.G. Baboul, B.B. Stefanov, G. Liu, A. Liashenko, P. Piskorz, I. Komaromi, R. Gomperts, R.L. Martin, D.J. Fox, T. Keith, M.A. Al-Laham, C.Y. Peng, A. Nanayakkara, M. Challacombe, P.M.W. Gill, B. Johnson, W. Chen, M.W. Wong, J.L. Andres, C. Gonzalez, M. Head-Gordon, E.S. Replogle, J.A. Pople, Gaussian 98, Revision A.11.1 Gaussian, Inc., Pittsburgh, PA, 2001.
[17] G. Maruta, S. Takeda, K. Yamaguchi, K. Ueda, T. Sugimoto, Synth. Met. 103 (1999) 2333.
[18] G. Maruta, S. Takeda, R. Imachi, T. Ishida, T. Nogami, K. Yamaguchi, J. Am. Chem. Soc. 121 (1999) 424.
[19] S. Yamanaka, T. Kawakami, S. Yamada, H. Nagao, M. Nakano, K. Yamaguchi, Chem. Phys. Lett. 240 (1995) 268.
[20] C. Heller, H.M. McConnell, J. Chem. Phys. 32 (1960) 1535.
[21] A. Carrington, A.D. McLachlan, Introduction to Magnetic Resonance, Harper & Row, New York, 1967.